Inorg. Chem. **2002**, *41*, 6856–6866

Polymethylated DOTA Ligands. 2. Synthesis of Rigidified Lanthanide Chelates and Studies on the Effect of Alkyl Substitution on Conformational Mobility and Relaxivity

Ramachandran S. Ranganathan,[†] Natarajan Raju,[†] Helen Fan,[†] Xun Zhang,[†] Michael F. Tweedle,*[,†] Jean F. Desreux,*[,‡] and Vincent Jacques[‡]

Ernst Felder Laboratories, Bracco Research USA, Inc., Princeton, New Jersey 08540, and Coordination and Radiochemistry, University of Liège, Sart Tilman B6, B-4000 Belgium

Received May 6, 2002

M4DOTA, [(2*S*,5*S*,8*S*,11*S*)-4,7,10-tris-carboxymethyl-2,5,8,11-tetramethyl-1,4,7,10-tetraazacyclododecan-1-yl]acetic acid (**2e**), and M4DOTMA, (*R*)-2-[(2*S*,5*S*,8*S*,11*S*)-4,7,10-tris-((*R*)-1-carboxyethyl)-2,5,8,11-tetramethyl-1,4,7,10-tetraazacyclododecan-1-yl]propionic acid (**3e**), are derivatives of ligand DOTA (**1e**) that form sterically crowded lanthanide chelates. M4DOTMA forms highly symmetric and totally rigid single Y^{3+} and Yb^{3+} species in which the ring substituents occupy corner positions in a square antiprismatic arrangement as shown by molecular mechanics calculations and by a quantitative interpretation of the relative magnitudes of the paramagnetic ^{1}H NMR shifts of dipolar origin. The NMR spectrum of $YbM4DOTMA^-$ displays two intense methyl peaks outside the 0–10 ppm range whose shift difference is strongly temperature dependent. $YbM4DOTMA^-$ (**3d**) could be a useful probe in magnetic resonance thermometric imaging. With only four methyl substituents on the tetraaza ring, M4DOTA forms three Yb^{3+} species in solution. The methyl substituents prevent the inversion of configuration of the ethylenic groups but not of the acetate arms. Although the methyl groups are likely to preferably occupy ring corner positions, the dipolar equations do not allow one to distinguish with certainty between the two available corner (equatorial) orientations. Reliably applying the dipolar equations is less obvious than usually assumed. A single methyl substituent as in ligand MDOTA (**5e**) suffices to rigidify the tetraaza cycle but not the acetate arms. Racemic $YbMDOTA^-$ (**5d**) is present in solution as four totally asymmetric topomers with the methyl groups occupying either one of the two equatorial positions. A complete assignment of the solution structures on the basis of the dipolar equations is again uncertain. The nuclear magnetic relaxation dispersion curves of the Gd^{3+} chelates of all the methylated DOTA ligands including DOTMA, (*R*)-2-[4,7,10-tris-((*R*)-carboxyethyl)- 1,4,7,10- tetraazacyclododecan-1-yl]propionic acid, are very similar, and intermolecular conformational processes appear to have no influence on the relaxivity of these small complexes for which the relaxation T_1 is mainly determined by the rotational correlation time (τ_r). The hydration number of the Tb^{3+} chelates measured by fluorescence decreases from DOTMA to M4DOTMA presumably because steric crowding leads to an increase of the metal–water distance.

Introduction

The use of gadolinium chelates has gained wide acceptance[1−3] in radiology as a means of increasing the contrast of tissues in magnetic resonance imaging (MRI). The contrast enhancement is due to the ability of the paramagnetic Gd^{3+} ion to shorten the T_1 and T_2 relaxation times of the protons of nearby water molecules (also expressed as relaxivities in s^{-1} mM^{-1}). Because Gd^{3+} itself is highly toxic (intravenous $LD_{50} \sim 0.2$ mmol/kg in mice), it must be administered as a chelate of exceptionally high thermodynamic stability and kinetic inertia, thus rendering the paramagnetic metal biologically tolerable ($LD_{50} \sim 10$ mmol/kg). Extensive

* Authors to whom correspondence should be addressed. E-mail: jf.desreux@ulg.ac.be (J.F.D.); Michael_F_Tweedle@bru.bracco.com (M.F.T.). Phone: +32(0)4.366.35.01 (J.F.D.). Fax: +32(0)4.366.47.36 (J.F.D.).
[†] Bracco Research USA, Inc.
[‡] University of Liège.

(1) Caravan, P.; Ellison, J. J.; McMurry, T. J.; Lauffer, R. B. *Chem. Rev.* **1999**, *99*, 2293−2352.
(2) Merbach, A. E.; Toth, E., Eds. *The chemistry of contrast agents in medical magnetic resonance imaging*; Wiley: Chichester, U.K., 2001.
(3) Kumar, K.; Tweedle, M. F. *Pure Appl. Chem.* **1993**, *65*, 515−520.

10.1021/ic025695e CCC: $22.00
Published on Web 11/15/2002

Scheme 1 [a]

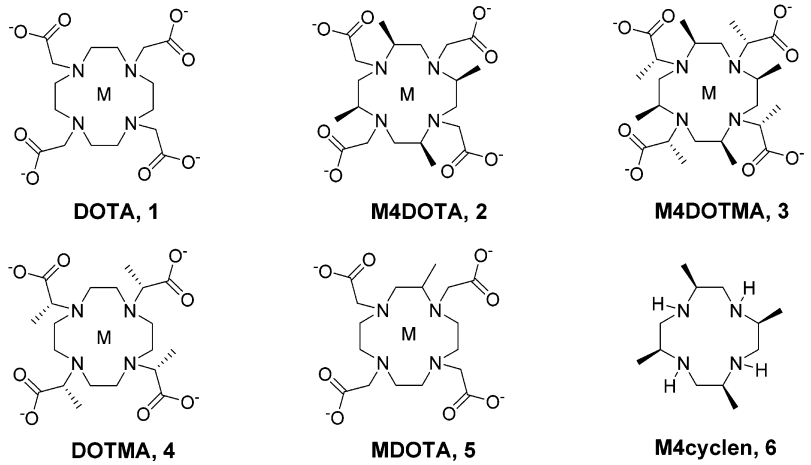

[a] a, M = Gd^{3+}; b, M = Tb^{3+}; c, M = Y^{3+}; d, M = Yb^{3+}; e, protonated ligand.

research and development have resulted in the introduction of effective and safe MRI contrast agents that are routinely used clinically. Notable examples are the ionic agents $Gd(DTPA)^{2-}$ and $Gd(DOTA)^{-}$ (**1a**, see Scheme 1) and the nonionic agents Gd(DTPA-BMA) and Gd(HPDO3A) that are used to define brain tumors and other morphologic abnormalities, large blood vessels, and excretory functions.[1−3] Despite these successes, many attempts have failed to extend contrast-enhanced MRI to finer biological processes exploiting receptor mediated targeting techniques. The low sensitivity ($\sim 3 \times 10^{-5}$ M) with which MRI detects Gd chelates poses a severe limitation for imaging biochemistry as receptors, and acceptors are present only in submicromolar to nanomolar concentrations. Hence, there is a need for more efficient Gd chelates.

The relaxation of water protons is a catalytic process, and so, it is amenable to chemical manipulation of the Gd−ligand−water system. Among the parameters that influence relaxivity (or longitudinal relaxation rate for a 1 mmol Gd(III) solution in s^{-1} mM^{-1}, vide infra), the one most limiting in the long run and the most difficult to characterize theoretically and chemically is the electronic relaxation of the Gd(III) ion in the chelate. It has been postulated[5,6] that increased symmetry and rigidity of the chelate structure will decrease the electronic relaxation rate, thus delivering greater relaxivity when the Gd chelates are bound to large biochemical structures. Specifically, high symmetry should increase the degeneracy of the energy states available to the unpaired electrons of the metal ion while greater rigidity should retard intraligand molecular fluctuations that distort the field at the metal center and decrease their magnitude. The rigidity of the DOTA ligands also influences the rate of association or dissociation of their metal chelates. A molecular modeling approach has recently been suggested that expresses rigidity of such molecules in qualitative terms.[4]

We decided to increase the rigidity of DOTA by substituting methyl groups on the macrocyclic carbon atoms and/or the carboxymethyl arms of the ligands while maintaining high symmetry. The synthesis and properties of the ligands [(2*S*,5*S*,8*S*,11*S*)-4,7,10-tris-carboxymethyl-2,5,8,11-tetramethyl-1,4,7,10-tetraazacyclododecan-1-yl]acetic acid, M4DOTA, **2e**, and (*R*)-[(2*S*,5*S*,8*S*,11*S*)-1,4,7,10-tris((*R*)-1-carboxyethyl)-2,5,8,11-tetramethyl-1,4,7,10-tetraazacyclododecan-1-yl]propionic acid, M4DOTMA, **3e**, have been reported in an earlier publication,[7] and the present paper will be entirely devoted to their lanthanide chelates. For comparison purposes, the complexes formed by *rac*-(4,7,10-tris-carboxymethyl-2-methyl-1,4,7,10-tetraazacyclododecan-1-yl)acetic acid, MDOTA, **5e**, have also been considered. An NMR investigation of the solution structure of the diamagnetic and paramagnetic lanthanide chelates will be reported first. The relaxation properties of the Gd^{3+} complexes will then be analyzed.

Experimental Section

$GdCl_3 \cdot 6H_2O$, $Gd(acetate)_3 \cdot 4H_2O$, $TbCl_3 \cdot 6H_2O$, $YCl_3 \cdot 6H_2O$, and $YbCl_3 \cdot 6H_2O$ were purchased from Sigma-Aldrich. $YbCl_3$ was hydrolyzed to $Yb(OH)_3$ by treatment with 1 N NaOH, and the hydroxide was filtered, washed with water till neutral, and then dried at 50 °C for 20 h at 0.5 mm Hg before use. Mass spectra were obtained from M-Scan, Inc. (West Chester, PA). Quantitative Technologies, Inc. (Whitehouse, NJ) provided elemental analysis data.

General Procedure for the Synthesis of the Metal Chelates. The MDOTA ligand was synthesized as reported by Schaeffer et al.[8] All the other methylated DOTA derivatives were prepared as described previously.[7] The experimental conditions and yields for the preparation of each metal chelate and the analytical data are summarized in Tables T1 and T2 in the Supporting Information. Typically, a 1 M NaOH solution was added to a solution of the ligand in deionized water (concentration 10 to 150 mM) to adjust the pH to 5.5. A solution of a lanthanide salt in deionized water, or, in the case of $Yb(OH)_3$, a suspension of the solid, was then

(4) Shukla, R.; Nunn, A. D.; Tweedle, M. F. *Magn. Reson. Med.,* submitted for publication.
(5) Aime, S.; Botta, M.; Ermondi, G.; Fedeli, F.; Uggeri, F. *Inorg. Chem.* **1992**, *31*, 1100−1103.
(6) Koenig, S. H. *Magn. Reson. Med.* **1991**, *22*, 183−190.
(7) Ranganathan, R. S.; Pillai, R. K.; Raju, N.; Fan, H.; Nguyen, H.; Tweedle, M. F.; Desreux, J. F.; Jacques, V. Submitted for publication.
(8) Schaefer, M.; Doucet, D.; Bonnemain, B.; Meyer, D. Europ. Pat. EP 287465, 1988.

added (using the excess specified in Table T1, concentration 35−100 mM). The pH of the mixture was maintained at the specified value by adding 1 N NaOH. Solutions that became slightly turbid upon addition of the alkali became clear upon heating. The solution was then stirred at high temperature for several hours as indicated in Table T1. The pH of the solution was adjusted to 9.0−9.5 by adding 1 M NaOH in order to precipitate the excess metal salt as the insoluble hydroxide (see Table T1 for conditions). The mixture was then filtered through a 0.22 μm filter and the pH of the filtrate adjusted to 7.0. The solution was concentrated and subjected to preparative HPLC as indicated in Table T2. The fractions were monitored by UV at 210 nm. The fractions containing the chelate were combined and then lyophilized to obtain the pure compound.

NMR Measurements and Computations. Spin−lattice relaxation time, T_1, measurements were carried out using the inversion−recovery method on an IBM PC/20 Multispec relaxometer (Bruker Ltd., Canada) operating at a fixed field of 0.47 T (20 MHz) at 40 ± 1 °C. The T_1 values of five GdL samples (concentrated 0.25−0.50 mM, Bis-Tris buffer, pH 7) were measured, and the slopes of the linear $(1/T_1)_{obsd}$ versus [GdL] plots were taken as r_1 values. The r_1 values are reported in Table T3 in the Supporting Information. NMR dispersion curves were recorded on a Stelar relaxometer (Mede, Italy) and on a field-cycling relaxometer described elsewhere.[9,10] The NMR spectra were recorded on an Avance DRX-400 spectrometer (Bruker) equipped with a temperature controller (±0.1 K). The COSY 2D spectra were typically recorded with 1024 data points in t_2 and 512 data points in t_1 with a bandwidth of 3−25 kHz. A 0° shifted sine bell apodization function was applied in both dimensions prior to the Fourier transformation. The EXSY experiments were performed using a phase sensitive pulse sequence with $2048t_2 \times 2048t_1$. Both dimensions were apodized by a 90° shifted sine bell function without zero filling. The mixing time t_m was 20 ms for the paramagnetic Yb^{3+} complexes. A 500 ms mixing time was used in the ROESY experiments with a 1024 × 512 data set. Zero-filling was applied to obtain a 1024 × 1024 size. Exchange and nOe cross-peaks were distinguished from one another on the basis of their sign, that is, respectively, identical or opposite to the sign of the diagonal peaks. The variable temperature unit was calibrated with ethylene glycol.

Molecular mechanics calculations were performed with the MM2 force field implemented in Chem 3D Pro v.5 (Cambridge Scientific Computing, Cambridge, MA) augmented with the parameters reported by Hay[11] and Cundari et al.[12] for the f elements.

Luminescence Measurements. The results of this study are given in Table T3 in the Supporting Information. The transient luminescence data were collected with a pulsed nitrogen laser-based luminescence apparatus. Two long-pass color filters, 475 and 535 nm, were placed between the 1 cm sample cell and the photomultiplier tube (PMT). A 1 ms initial delay was used to bypass fast fluorescence emissions, if any, and to allow the PMT to recover from possible saturation caused by scattered excitation. The emission decay rate constants were obtained by least-squares fitting of the decay curves into single-exponential functions. The pH of the sample solutions was varied between 4 and 10, with the transient luminescence measurement being made at each pH reading. The acidity of the D_2O solutions was also varied by adding standard NaOD or DCl. The luminescence decay rate constants of the Tb complex in H_2O and D_2O solutions, k_{H_2O} and k_{D_2O}, at various pH/pD values were used to calculate the inner-sphere water coordination number, q_{water}, on the basis of the equation $q_{water} = A(k_{H_2O} - k_{D_2O} - 0.06)$ where A is a proportionality constant assumed to be 5 ms on the basis of previous luminescence and crystallographic studies of various Tb(III) complexes.[13,14]

Results and Discussion

The Gd^{3+}, Tb^{3+}, Y^{3+}, and Yb^{3+} chelates, **2a**−**d**, **3a**−**d**, were prepared using the standard procedure described in the Experimental Section (see Table T1 in the Supporting Information). The rates of formation of these chelates were slower than those of DOTA, **1**, and generally required higher temperatures and more basic pH conditions as well as longer reaction times. These chelates were purified by reversed phase preparative HPLC. The isolated yields of the pure chelates were generally lower than those obtained for the chelates belonging to the less rigid DOTA ligand. The analytical data for the chelates are summarized in Table T2 in the Supporting Information. The mass spectral and elemental analysis data were in full agreement with the structures assigned to these chelates, and the greatest care was taken to prepare highly pure compounds. As expected, the reversed phase HPLC retention times of the new chelates were longer than those of the corresponding DOTA complexes reflecting their greater hydrophobicity due to substitutions by four or eight methyl groups.

NMR Studies of the Y^{3+} and Yb^{3+} Chelates. The NMR spectra of the lanthanide DOTA chelates have been investigated in great detail.[2,15−18] The remarkably high thermodynamic stability and kinetic inertness of these chelates have been assigned to the steric requirements of the DOTA ligand and to the close fit between the cavity formed by its donor atoms and the trivalent lanthanide ions. The tetraazacyclododecane ring adopts one of its most stable conformations, a [3.3.3.3] square arrangement of 4-fold symmetry in which all ethylenic groups are fully staggered.[15−18] Moreover, the nitrogen and oxygen donor atoms form a nearly perfect square antiprism that is a geometric arrangement known to have a minimum repulsion energy coefficient.[19] This tight packing of the ligand does not prevent all the ethylenic groups from adopting simultaneously either a δ or a λ conformation nor the carboxylic groups from rotating around the $N-CH_2-COO^-$ bonds. The carboxylic groups form either a clockwise (Λ) or a counterclockwise (Δ) four-bladed propeller-like arrangement, and the tetraaza ring displays either a clockwise or counterclockwise helicity labeled $\lambda\lambda\lambda\lambda$

(9) Vander Elst, L.; Maton, F.; Laurent, S.; Seghi, F.; Chapelle, F.; Muller, R. N. *Magn. Reson. Med.* **1997**, *38*, 604−614.
(10) Koenig, S. H.; Brown, R. D. *Prog. Nucl. Magn. Reson. Spectrosc.* **1990**, *22*, 487−567.
(11) Hay, B. P. *Inorg. Chem.* **1991**, *30*, 2876−2884.
(12) Cundari, T. R.; Moody, E. W.; Sommerer, S. O. *Inorg. Chem.* **1995**, *34*, 5989−5999.
(13) Beeby, A.; Clarkson, I. M.; Dickins, R. S.; Faulkner, S.; Parker, D.; Royle, L.; de Sousa, A. S.; Williams, J. A. G.; Woods, M. *J. Chem. Soc., Perkin Trans. 2* **1999**, 493−503.
(14) Horrocks, W. D. J.; Sudnick, D. R. *J. Am. Chem. Soc.* **1979**, *101*, 334−340.
(15) Desreux, J. F. *Inorg. Chem.* **1980**, *19*, 1319−1324.
(16) Jacques, V.; Desreux, J. F. *Inorg. Chem.* **1994**, *33*, 4048−4053.
(17) Aime, S.; Botta, M.; Fasano, M.; Marques, M. P. M.; Geraldes, C. F. G. C.; Pubanz, D.; Merbach, A. E. *Inorg. Chem.* **1997**, *36*, 2059−2068.
(18) Aime, S.; Botta, M.; Ermondi, G. *Inorg. Chem.* **1992**, *31*, 4291−4299.
(19) Kepert, D. L. *Inorganic stereochemistry*; Springer-Verlag: Berlin, 1982.

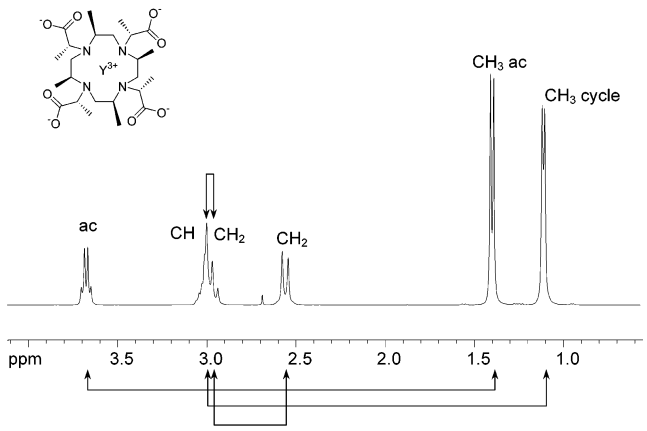

Figure 1. ^{1}H spectrum of the Y^{3+} complex of M4DOTMA, **3c**, at room temperature. The COSY connections are indicated below the spectrum.

or $\delta\delta\delta\delta$. Two diastereomers result from these spatial arrangements, each being present as an enantiomeric pair, $\Delta(\lambda\lambda\lambda\lambda)$ and $\Lambda(\delta\delta\delta\delta)$ on one hand and $\Lambda(\lambda\lambda\lambda\lambda)$ and $\Delta(\delta\delta\delta\delta)$ on the other.[17−18] These diastereomers give rise to separate resonances that can cover a wide chemical shift range if the encapsulated metal ion is paramagnetic. They differ by the angle α between the diagonals of the parallel squares formed by the four nitrogen atoms and the four carboxylic oxygen atoms of DOTA. Values of about $\alpha = 35°$ and $\alpha = -15°$ have been found in crystallographic structures and have been compared to the values defining a perfect square antiprism ($\alpha = +45°$) and a perfect prism ($\alpha = 0°$). A square antiprismatic geometry is obtained for a $\Lambda(\delta\delta\delta\delta)$ or a $\Delta(\lambda\lambda\lambda\lambda)$ arrangement, that is, an opposite helicity of the tetraaza ring and of the acetate arms, while the forms with same ring and acetate helicity, $\Lambda(\lambda\lambda\lambda\lambda)$ and $\Delta(\delta\delta\delta\delta)$, lead to a pseudoprismatic structure also called twisted antiprismatic.[17−18] Intramolecular exchanges have been observed in the EXSY spectra for each diastereomer of $YbDOTA^-$ in addition to intermolecular exchanges between the diastereomers.[16,17] These exchanges are accelerated by raising the temperature, and all peaks of $LaDOTA^-$ and of $YbDOTA^-$ become extremely broad at about 290 and 350 K, respectively.

The spectral properties of the diamagnetic Y^{3+} and the paramagnetic Yb^{3+} chelates of M4DOTMA, M4DOTA, and MDOTA are investigated in the present paper. The properties of the Y^{3+} ion are quite close[20] to those of the later lanthanides Er^{3+} and Ho^{3+}, and the present NMR study is thus devoted to two very similar metal chelates. This analysis follows an order of increasing complexity of the NMR spectra and starts with the M4DOTMA chelates.

M4DOTMA Chelates. The M4DOTMA ligand, **3e**, features four methyl substituents on the tetraaza ring and on the acetate arms in the *SSSS* and *RRRR* configurations, respectively. Its metal chelates are expected to be highly rigid and symmetric. The ^{1}H spectrum of $YM4DOTMA^-$, **3c**, features only six peaks as expected for a chelate of 4-fold symmetry (Figure 1, COSY connections shown at the bottom of this Figure, see also Figure S1 in the Supporting Information). This spectrum is identical at room temperature and at 358 K: the couplings remain unaltered, and the peak half-widths decrease somewhat upon raising the temperature (from 33 Hz at 278 K to 16 Hz at 350 K). A complete assignment is readily made on the basis of the coupling patterns, the relative peak areas, and the COSY spectrum. The methyl groups appear as two doublets each of relative area 3. As indicated at the bottom of Figure 1, the resonance at 1.4 ppm is linked by a COSY connection to a quadruplet at 3.67 ppm (area 1) that shows no connection with any other resonance. These peaks are thus assigned to the acetate methyl and methine groups, respectively. Moreover, the methyl resonance at high field (1.11 ppm) is due to the methyl groups on the tetraaza ring as it is coupled to the complex pattern at ~3 ppm and to a resonance at 2.55 ppm originating from the cycle. The ring methyl groups can be located either in an equatorial or an axial position. An equatorial orientation is expected as the axial positions are excessively crowded even in the free ligands.[7] An equatorial orientation of the methyl groups would be characterized by one large ^2J, one large $^3J_{ax-ax}$, and one small $^3J_{ax-eq}$, while an axial orientation would lead to one large ^2J and two small ^3J as shown by the Karplus equation.[21] The methylene protons next to a methyl group in an equatorial orientation thus appear as two doublets of doublets. The spectrum of $YM4DOTMA^-$ could be simulated with the ring methyl groups in the equatorial position with $^2J = -14.1$ Hz, $^3J_{ax-ax} = 11.9$ Hz, and $^3J_{ax-eq} = 0.75$ Hz plus small coupling constants (~0.6 Hz) with the methyl group (Figure S2). Similar J constants were used earlier[7] to simulate the NMR spectrum of the unsubstituted macrocycle (2*S*,5*S*,8*S*,11*S*)-2,5,8,11-tetramethyl-1,4,7,10-tetraazacyclododecane (**6**) and yielded two well resolved doublets of doublets for the methylene protons as expected. However, the chemical shift of the axial methylene proton of amine **6** is smaller than the shift of the methylene equatorial proton while the opposite is found for $YM4DOTMA^-$. The unusual coupling pattern of the resonance at 2.5 ppm stems from this shift reversal.

Scheme 2

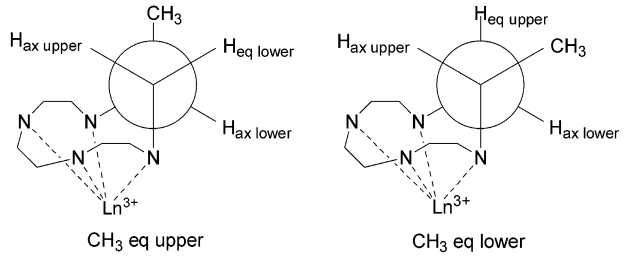

As illustrated in Scheme 2, the equatorial methyl groups can be located in two different positions relative to the tetraaza ring. These positions will be labeled "eq upper" or "eq lower", and a distinction between them is possible when investigating the NMR spectra of paramagnetic chelates. As in the case of DOTA,[15−17] an investigation of the paramagnetic chelates is indeed very informative. The analysis will

(20) Cotton, F. A.; Wilkinson, G.; Murillo, C. A.; Bochmann, M. *Advanced inorganic chemistry*; Wiley: New York, 1999.

(21) Contreras, R. H.; Peralta, J. E. *Prog. Nucl. Magn. Reson. Spectrosc.* **2000**, *37*, 321−425.

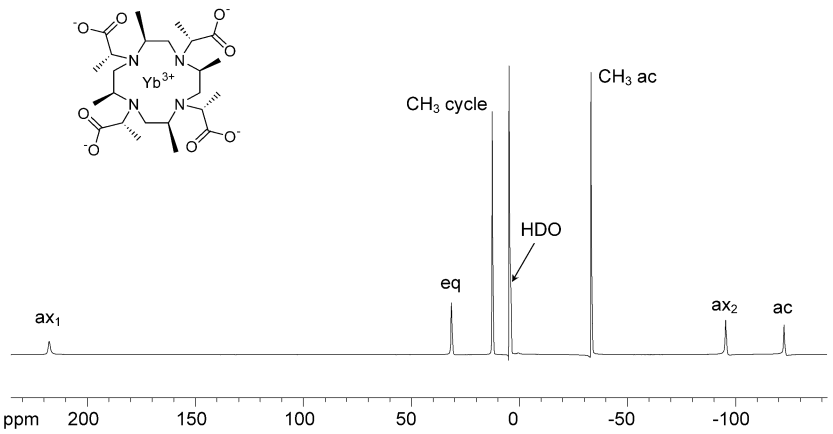

Figure 2. ^{1}H spectrum of the Yb^{3+} complex of M4DOTMA, **3d**, at room temperature.

be restricted to the M4DOTMA complex with Yb^{3+}, **3d**, as the latter is known to induce large paramagnetic shifts that essentially originate from through space interactions between the ligand nuclei and the unpaired electronic spins of the metal ion.[2] Provided the complex is axially symmetric (C_3 or above), the relative magnitudes of the NMR shifts induced by Yb^{3+} yield information on the solution structure because they depend on a simple geometric factor and on a magnetic susceptibility term D_{ax}

$$\delta_i = D_{ax}\left\langle \frac{3\cos^2\theta_i}{r_i^3} \right\rangle \qquad (1)$$

where θ_i and r_i are the polar coordinates of nucleus i in the set of axes of the susceptibility tensor that is oriented with the main symmetry axis.[22] The D_{ax} term is a characteristic of the complex and is identical for all nuclei. The agreement between the experimental paramagnetic shifts and the shifts computed from a structural model is usually estimated by computing the R factor[15]

$$R = \sqrt{\frac{\sum_{i=1}^{n}(\delta_{icalcd} - \delta_{iexpt})^2}{\sum_{i=1}^{n}(\delta_{icalcd})^2}} \qquad (2)$$

The ^{1}H spectrum of $YbM4DOTMA^-$, **3d**, is reproduced in Figure 2. This spectrum covers approximately 350 ppm and is very nicely resolved into six peaks as expected for a single species of 4-fold symmetry (plus the water peak at 5 ppm). The peaks are easily assigned by comparison with the spectrum of $YbDOTA^-$ (**1d**). Dipolar geometric factors were calculated starting from the solid state structure of either antiprismatic $EuDOTA^-$ [15] or twisted antiprismatic $LaDOTA^-$ [18] modified by the addition of methyl groups in the tetraaza ring and on the acetate functions in the *SSSS* and *RRRR* configurations, respectively. The structures were minimized in the gas phase using the parameters reported by Hay[11] and by Cundari et al.[12] for the Yb^{3+} complexes. After minimizing the antiprismatic structure with the methyl groups in the "eq upper" position, the twist angle α between the N_4 and O_4 faces remained essentially unchanged (α = 34.2°), and an excellent agreement (R = 3.1%) was found between the experimental and calculated paramagnetic shifts (Figure S3, D_{ax} = 6420 ppm Å^{-3}). Using the twisted antiprismatic $LaDOTA^-$ structure after optimization (twist angle α = 21°) as a model led to a poor agreement factor (R = 26.3%). Particularly large differences were found between the calculated and experimental shifts of the resonances at high fields. Poor R values were also computed if all the ring methyl groups were oriented in "eq lower" positions whether in a square antiprismatic (R = 15.2%) or in a twisted antiprismatic geometry (R = 29.1%). The differences between the R factors appear sufficiently large to reliably assign a pseudoantiprismatic geometry to $YbM4DOTMA^-$, **3d**. Computing the relative energies of the various topomers of a lanthanide chelate derived from DOTA requires advanced ab initio and molecular mechanics methods as well as techniques to take solvation effects into account[23−25] that are beyond the scope of the present paper. However, some confidence can be lent to calculations on $YbM4DOTMA^-$ because of the excessive steric crowding of this chelate. The relative energies computed by molecular mechanics at the MM2 level with the parameters suggested by Hay[11] and Cundari et al.[12] yielded 0.0 (reference), 9.3, 14.9, and 17.4 kcal/mol for the square antiprism "eq upper" and "eq lower", and twisted square antiprism "eq upper" and "eq lower", respectively. The axial positions are so crowded as to render calculations meaningless. These computations are in agreement with the NMR studies, and the differences in energies are sufficiently large to support the presence of only one species in solution.[26] The computed structure of $YbM4DOTMA^-$ is presented in Figure 3. As expected, the

(22) Forsberg, J. H. NMR studies of paramagnetic lanthanide complexes and shift reagents. In *Handbook on the physics and chemistry of rare earths*; Gschneidner, K. A., Jr., Eyring, L., Eds.; North-Holland Elsevier: Amsterdam, 1998; pp 1−68.

(23) Cosentino, U.; Moro, G.; Pieta, D.; Villa, A.; Fantucci, P. C.; Maiocchi, A.; Uggeri, F. *J. Phys. Chem.* **1998**, *102*, 4606−4614.

(24) Henriques, E. S.; Bastos, M.; Geraldes, C. F. G. C.; Ramos, M. J. *Int. J. Quantum Chem.* **1999**, *73*, 237−248.

(25) Varnek, A.; Wipff, G.; Bilyk, A.; Harrowfield, J. M. *J. Chem. Soc., Dalton Trans.* **1999**, 4155−4164.

(26) Comba, P.; Hambley, T. W. *Molecular modeling of inorganic compounds*; Wiley-VCH: Weinheim, 2001.

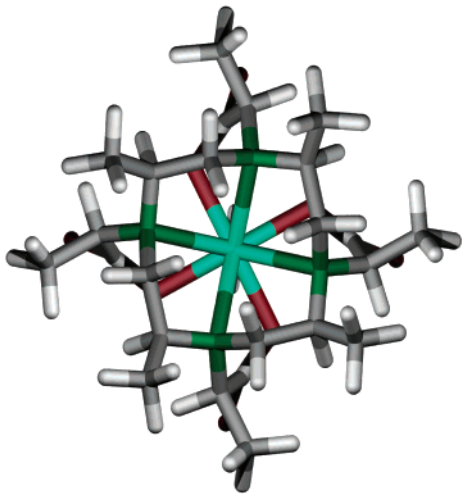

Figure 3. Model of the most stable geometry of YbM_4DOTMA^-, **3d**, as deduced from NMR studies and molecular mechanics calculations.

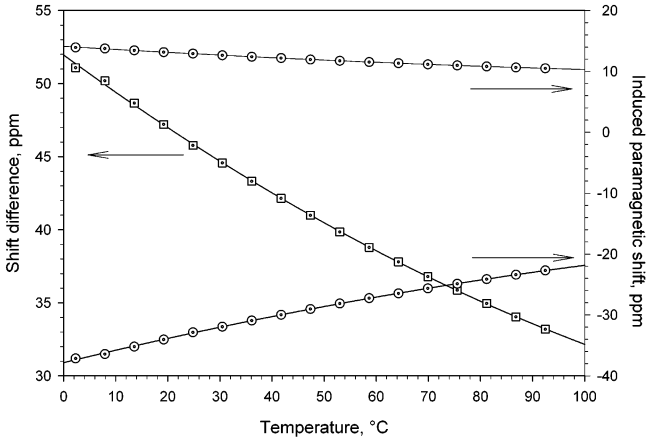

Figure 4. Temperature dependence of the NMR shifts of the two methyl resonances of YbM4DOTMA$^-$, **3d**, (right axis) and of the difference between these shifts (left axis).

methyl groups are as far apart as possible and occupy corner positions that are indeed known to be the most unhindered in medium size rings.[27]

The ^{1}H spectrum of YbM4DOTMA$^-$ features two intense methyl peaks that are outside the normal 0−10 ppm proton NMR shift range. The shift difference $\Delta\delta$ between these two peaks is strongly temperature dependent as shown in Figure 4 and obeys the experimental law

$$\Delta\delta = 51.95 - 0.26 \times T + 6.32 \times 10^{-4} \times T^2 \quad (T \text{ in } °\text{C})$$

with $r^2 = 0.9996$. Lanthanide chelates of M4DOTMA could thus be used as in vivo NMR thermometers, for instance, for monitoring the hypothermia treatment of tumors and more generally for determining the temperature of body tissues by in vivo spectroscopy. This application of paramagnetic chelates has already been reported by Aime et al.[28] who used the Yb^{3+} chelate of DOTMA, **4d**, for determining temperature and by Roth et al.[29] and Sherry et al.[29] who suggested the Pr^{3+} and Tm^{3+} complexes of DOTA derivatives for the same purpose. The M4DOTMA chelates have a distinct advantage in that the temperature is deduced from the shift difference between two intense methyl peaks rather than from two small resonances[28] or even from the temperature dependence of a single resonance.[29]

M4DOTA Chelates. Two topomers are observed in the ^{1}H and ^{13}C spectra of the yttrium complex of (*R*,*R*,*R*,*R*)-M4DOTA, **2c** (see Figures 5 and S4). The ^{13}C spectrum displays five peaks for each form as expected for chelates of 4-fold symmetry. Several peaks are overlapping in the ^{1}H spectrum, but the analysis is greatly facilitated by the COSY spectrum (Figure S5) that clearly shows the coupling patterns between the different protons. The peak assignments indicated in Figure 5 are also borne out by the HMQC and NOESY spectra (Figures S6 and S7). The acetate protons of the major and minor forms appear as single AB forms at ∼3.4 and ∼3.1 ppm, respectively. Moreover, the ring protons of the minor form resonate at 2.6 and 2.8 ppm and appear as two doublets of doublets with, respectively, two large and one large and one small coupling constant. The same pattern was found in the ^{1}H spectrum of the free M4DOTA ligand and was assigned to an equatorial orientation of the methyl groups[7] in keeping with the coupling constants expected for this orientation. Analyzing the resonances of the major topomer of YM4DOTA$^-$ is less obvious because of peak overlappings, but the resonance at 2.21 ppm has the same unusual appearance of the methylene peak found at 2.55 ppm in the ^{1}H spectrum of YM4DOTMA$^-$. The spectrum was simulated with *J* constants and chemical shifts very similar to those calculated for this chelate (Figure S8; $^2J = -15.1$ Hz, $^3J_{ax-ax} = 13.2$ Hz, and $^3J_{ax-eq} = 3.4$ Hz). The major peaks are thus assigned to a geometric arrangement in which the methyl groups are located on the edges of a [3.3.3.3] conformation in an "eq upper" position as already observed for YM4DOTMA$^-$, **3c**. An "eq lower" orientation is assigned to the methyl groups of the minor isomer. Additional information is afforded by an analysis of the NMR spectra of YbM4DOTA$^-$.

The ^{1}H spectrum of YbM4DOTA$^-$, **2d**, (Figure 6) displays resonances that are attributed to three topomers in the ratio 1:0.095:0.013 at room temperature. These topomers are labeled M, m, and m′, respectively. The peaks of the major topomer are the most shifted and cover about 270 ppm. The M and m species give rise to six resonances as expected for chelates of 4-fold symmetry. Four or five resonances only are found for the m′ species depending on the temperature. Some resonances are probably hidden under more intense peaks. The peaks are assigned by comparison with the spectrum of YbDOTA$^-$ and by taking their relative areas into account. When the temperature is raised, the peaks assigned to the M and m species broaden, and eventually, the m peak disappears in the baseline at 353 K. Enlarged M resonances are still clearly visible at that temperature. However, the peak widths of the m′ resonances remain

(27) Dale, J. *Acta Chem. Scand.* **1973**, *27*, 1149−1158.
(28) Aime, S.; Botta, M.; Fasano, M.; Terreno, E.; Kinchesh, P.; Calabi, L.; Paleari, L. *Magn. Reson. Med.* **1996**, *35*, 648−651.
(29) Roth, K.; Bartholomae, G.; Bauer, H.; Frenzel, T.; Kossler, S.; Platzek, J.; Raduchel, B. E.; Weinmann, H. J. *Angew. Chem., Int. Ed. Engl.* **1996**, *35*, 655−657. See also Zuo, C. S.; Mahmood, A.; Sherry, A. D. *J. Magn. Reson.* **2001**, *151*, 101−106.

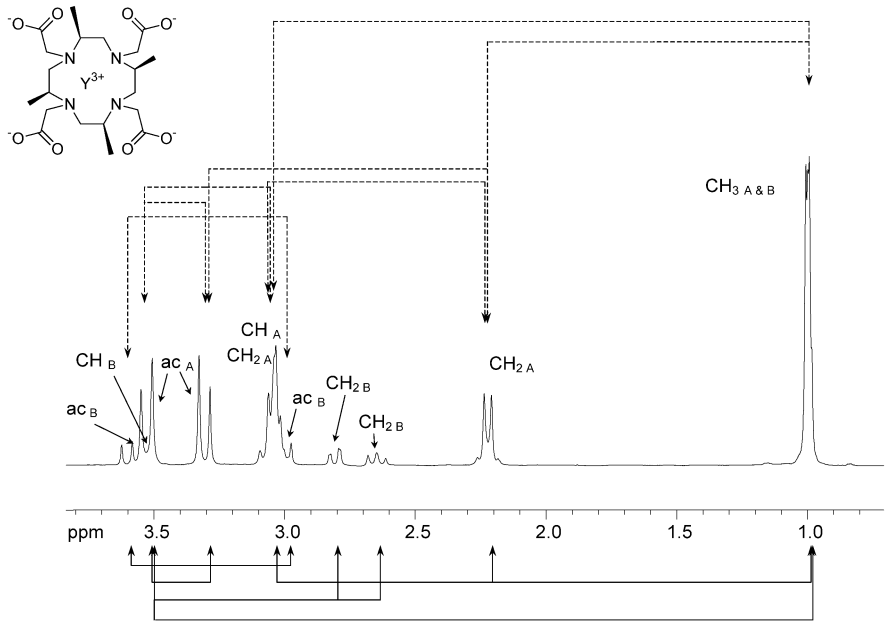

Figure 5. ^{1}H spectrum of the Y^{3+} complex of M4DOTA, **2c**, at room temperature. The COSY (—) and NOESY (- - -) connections are indicated below and above the spectrum, respectively.

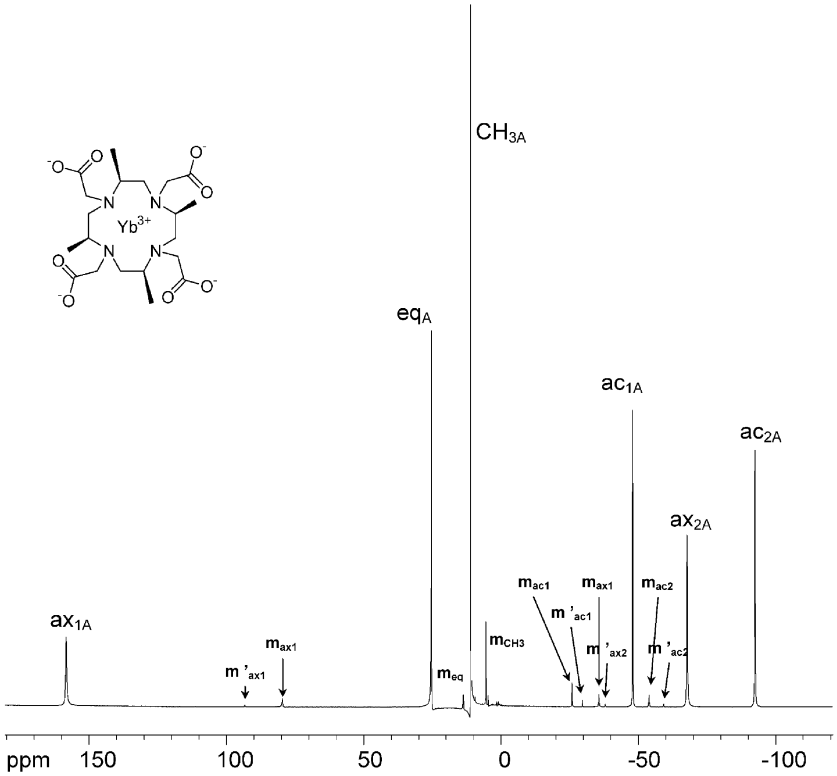

Figure 6. ^{1}H spectrum of the Yb^{3+} complex of M4DOTA, **2d**, at 283 K.

essentially unaltered (Figure S9). Recording NOESY spectra was thwarted by technical difficulties, and it was difficult to obtain sufficiently narrow diagonal peaks (Figure S10). However, exchange cross-peaks could be found between the M and m peaks in a few cases: $ax_{1M} \leftrightarrow ax_{1m}$, $CH_{3M} \leftrightarrow CH_{3m}$, $eq_M \leftrightarrow eq_m$, $ac_{1m} \leftrightarrow ac_{2M}$, and $ax_{2m} \leftrightarrow ax_{2M}$ on going from low to high fields. Moreover, no cross-peaks could be found between resonances arising from the same isomer, either M or m. The m′ resonances are obviously too small to allow the observation of exchange peaks should any be present. Exchanges are thus observed between M and m protons with the same orientation in the tetraaza cycle and between acetate protons in different locations. Consequently, the macrocyclic ring is rigid at the NMR time scale, but an inversion of the conformation of the acetate groups is taking place. Exactly the opposite dynamic behavior was reported by Aime et al.[30] for the lanthanide chelates of a DOTA ligand featuring a bulky nitrophenyl substituent on one of the acetate arms. In

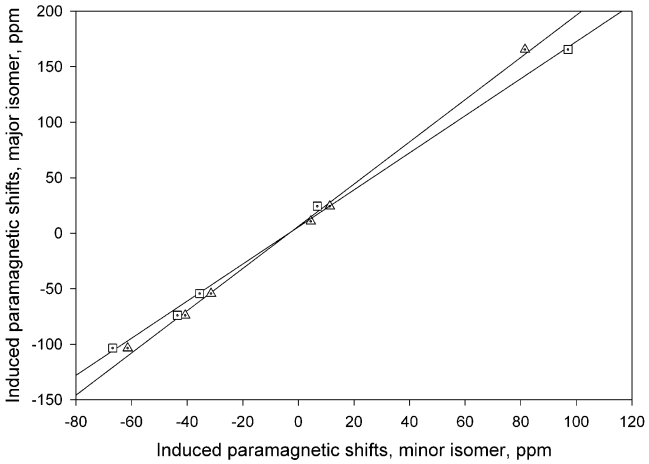

Figure 7. Correlation between the paramagnetic shifts of the major M and the minor m (dotted triangle) or m′ (dotted square) isomers of YbM4DOTA$^-$, **2d**.

that case, the conformation of the tetraaza cycle rapidly inverts, but the acetate arms are rigid, and EXSY cross-peaks thus appear between the M and m forms for axial−equatorial exchanges in the macrocyclic ring and for acetate protons in the same orientation. In keeping with the analysis of YM4DOTMA$^-$, the methyl groups of the M form of YbM4DOTA$^-$ are assigned an "eq upper" orientation with the acetate arms in Λ conformation in a square antiprismatic arrangement. The m species features the same orientation of the methyl substituents, but it adopts a twisted antiprismatic geometry with the acetate arms in a Δ conformation. The m′ isomer would then feature methyl groups in the "eq lower" orientation. This isomer would be sterically so crowded that either it would adopt one conformation only, presumably a square antiprismatic arrangement, or the motion of the acetate arms would already be rapid compared to the observation time at 275 K. Evaluations of the conformational energies of the various isomers of YbM4DOTA$^-$ require advanced ab initio or molecular dynamics computations[23−25] that are beyond the scope of the present paper, but one could expect that a calculation of the dipolar paramagnetic shifts would allow a distinction between the geometries of the different isomers. Figure 7 illustrates a difficulty of this approach that has been recently stressed[31,32] for the DOTMA chelates: an excellent correlation is found between the induced paramagnetic shifts of the major M and the minor m or m′ forms ($r^2 = 0.998$ and 0.996, respectively), and a distinction between these forms using eq 1 appears illusory even if several authors including us have attempted such a distinction in other cases[33,34] (the correlations however are good indications that the m′ resonances are not due to an impurity). The limitations of eq 1 are confirmed by calculations of the agreement factors *R* (eq 2): for instance, using an antiprismatic YbM4DOTA$^-$ energy-minimized model with the methyl groups in the "eq upper" orientation, *R* values of 2.6%, 10.1%, and 6.4% were calculated for the M, m, and m′ isomers, respectively. Although one could lend some significance to these *R* values, it is not believed that small differences between them can be reliably related to structural modifications. The situation is even more paradoxical because the correlations between the experimental and the calculated paramagnetic shifts of YbM4DOTA$^-$ in the square antiprismatic arrangement are nearly as good whether the methyl groups are in the "eq upper" (Figure S3, $R = 2.6\%$) or in the "eq lower" positions ($R = 6.6\%$). The geometric factors computed in eq 1 for the two orientations of the methyl groups are not very different, and structural inferences made on the basis of only the NMR spectra of the paramagnetic species must thus be accepted with reservation.

MDOTA Chelates. The same conclusion is reached in an investigation of the Yb^{3+} chelate **5d** of MDOTA, **5e**. This ligand was obtained as a racemic mixture by a synthetic procedure reported by Schaeffer et al.[8] Two enantiomeric pairs are expected for each orientation of the methyl group in YbMDOTA$^-$. Indeed, the chelate can adopt a square antiprismatic or a twisted square antiprismatic geometry. Moreover, in a square antiprismatic arrangement, the Δ($\lambda\lambda\lambda\lambda$) form with the methyl group in the *R* configuration is the enantiomer of the Λ($\delta\delta\delta\delta$) form with the methyl group in the *S* configuration (the same is true for Λ ($\lambda\lambda\lambda\lambda$) and Δ($\delta\delta\delta\delta$) in a twisted structure). The ^{1}H spectrum of YbMDOTA$^-$ is shown in Figure 8, and the COSY and EXSY spectra are reproduced in Figures S11−13. The presence of a single methyl group in YbMDOTA$^-$ is sufficient to cancel all degeneracies, and each proton in the ligand gives rise to a separate resonance (with some overlappings). The particularly large number of resonances and the 2D spectra are in agreement with the presence in solution of four totally asymmetric topomers that display exchange peaks connecting them two by two. The spectra are more easily interpreted by focusing on the most shifted peaks at low fields that correspond to the "axial upper" protons in the tetraaza ring (Figure 9). The four major peaks between 120 and 140 ppm give rise to exchange cross-peaks with the four minor peaks in the 70−100 ppm shift range, and the major resonances in that same shift range are exchanging with the minor resonances found at the highest fields. These exchanges connect protons in the same "axial upper" location in different topomers. On the contrary, exchanges are taking place between acetate protons in two different locations as shown in Figure S13. One single methyl group is thus able to prevent the ring inversion, and the exchange between diastereomers is again due only to a conformational rearrangement of the acetate arms. The increase in rigidity brought about by the addition of one methyl group to the DOTA structure is in agreement with the molecular modeling studies of Reichert et al.[35] who compared the Gd(III) complexes of DOTA and MDOTA. In line with the previous analyses in the present paper, the

(30) Aime, S.; Botta, M.; Ermondi, G.; Terreno, E.; Anelli, P. L.; Fedeli, F.; Uggeri, F. *Inorg. Chem.* **1996**, *35*, 2726−2736.
(31) Di Bari, L.; Pintacuda, G.; Salvadori, P. *Eur. J. Inorg. Chem.* **2000**, 75−82.
(32) Di Bari, L.; Pintacuda, G.; Salvadori, P.; Dickins, R. S.; Parker, D. *J. Am. Chem. Soc.* **2000**, *122*, 9257−9264.
(33) Brittain, H. G.; Desreux, J. F. *Inorg. Chem.* **1984**, *23*, 4459−4466.
(34) Zhang, S.; Kovacs, Z.; Burgess, S.; Aime, S.; Terreno, E.; Sherry, A. D. *Chem. Eur. J.* **2001**, *7*, 288−296.
(35) Reichert, D. E.; Hancock, R. D.; Welch, M. J. *Inorg. Chem.* **1996**, *35*, 7013−7020.

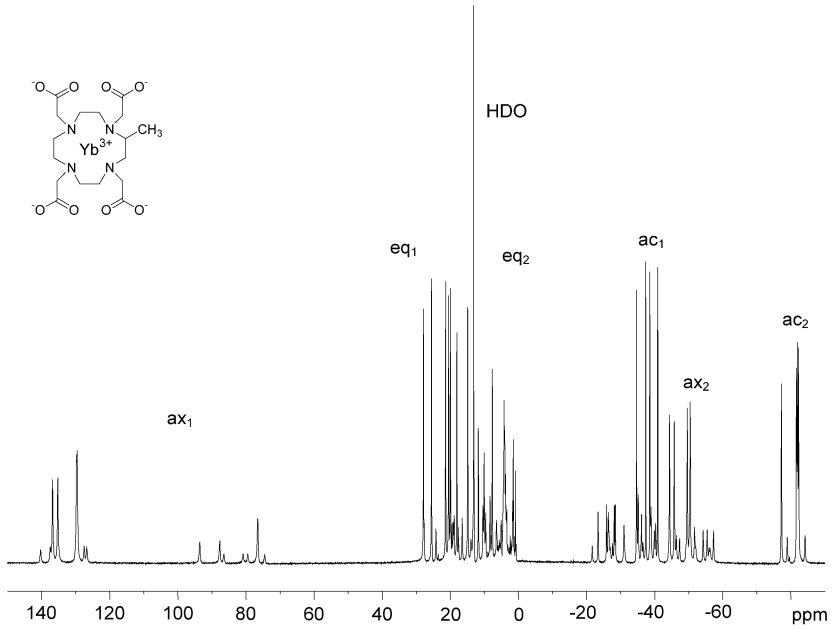

Figure 8. ^{1}H spectrum of the Yb^{3+} complex of MDOTA, **5d**, at 293 K.

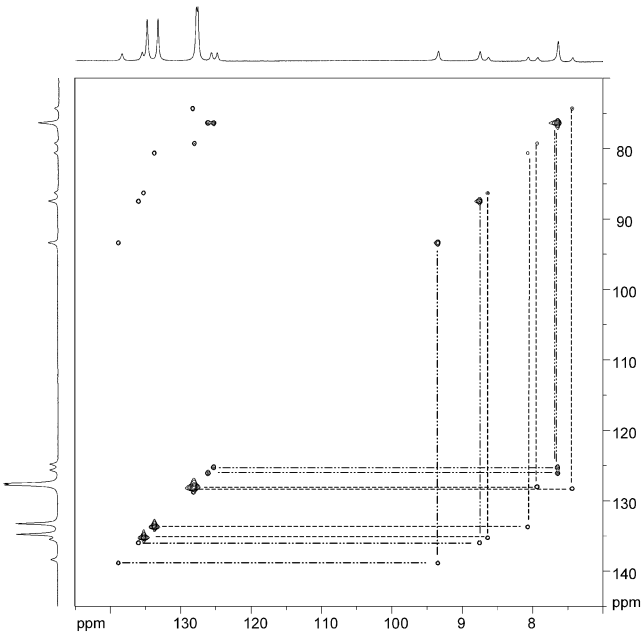

Figure 9. EXSY spectrum of the low field part of the ^{1}H spectrum of the Yb^{3+} complex of MDOTA, **5d**, at 293 K. The dashed (- - -) and dotted−dashed (−···−) lines link two resonances that are connected by exchange cross-peaks. These connections are examples of exchanges between topomers with a square antiprismatic or a twisted square antiprismatic geometry and with the methyl group in the "eq upper" or "eq lower" position, respectively (see text).

methyl group in $YbMDOTA^-$ is assumed to be oriented in the "eq upper" or "eq lower" position, the acetate arms being in either a clockwise or a counterclockwise propeller arrangement. Our MM2 computations indicate that $YbMDOTA^-$ in the square antiprismatic geometry with a methyl group in the "eq upper" position is the least crowded structure, and accordingly, it is assumed that the major peaks around 140 ppm originate from this arrangement while the minor peaks around 90 ppm are due to a reorientation of the acetate arms to a twisted geometry. The major peaks in the 70−90 ppm range would then be assigned to $YbMDOTA^-$ in the twisted conformation with its methyl group in the "eq lower" position. Inverting the layout of the acetate groups in this topomer would lead to the minor resonances in the 120−140 ppm range. One should not expect that MM2 computations could account for subtle structural differences such as the ones found in the case of $YbMDOTA^-$ even if Hay[11] and Cundari[12] parameters are used. The quantitative analysis of the induced paramagnetic shifts is not more informative. As shown in Figure S14, excellent correlations between experimental and calculated shifts are obtained for the most shifted major resonances using a square antiprismatic structure with a methyl group in either an "eq upper" or "eq lower" orientation. These correlations were obtained after orienting the axes of the susceptibility tensor in the full dipolar equation

$$\delta_i = D_{\mathrm{ax}}\left\langle \frac{3\cos^2\theta_i}{r^3}\right\rangle + D_{\mathrm{rh}}\left\langle \frac{\sin^2\theta_i\cos 2\varphi_i}{r^3}\right\rangle \qquad (3)$$

so as to obtain the best agreement with experiment (r_i, θ_i, and ϕ_i are the polar coordinates of nucleus i with respect to the principal directions of the magnetic susceptibility tensor whose axial and rhombic anisotropy parameters are D_{ax} and D_{rh}). A very small tilt of the Z axis (~2°) is enough to account for the relative magnitude of all the paramagnetic shifts after full assignment from the EXSY and COSY spectra.

Despite the extensive use of eqs 1−3 in the literature, it thus seems that interpreting quantitatively the relative magnitudes of the paramagnetic shifts can be fraught with difficulties in terms of satisfactory, reliable structural results. Protons in quite different locations can have very similar geometric factors as illustrated here for the Yb^{3+} chelates

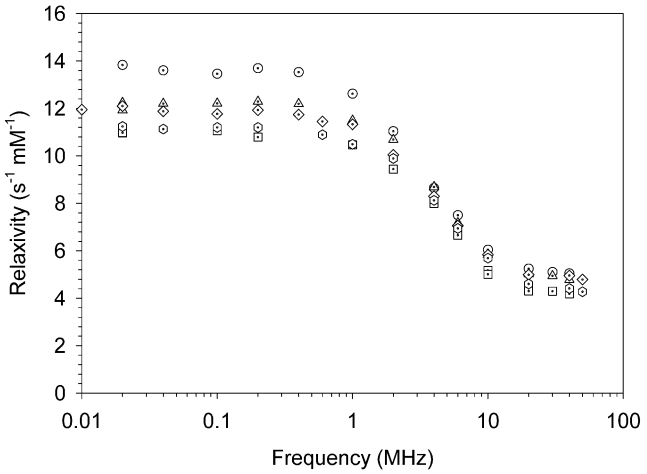

Figure 10. Nuclear magnetic relaxation dispersion curves of GdDOTA$^-$, **1a** (dotted hexagon), GdM4DOTMA$^-$, **3a** (dotted triangle), GdM4DOTA$^-$, **2a** (dotted circle), GdDOTMA$^-$, **4a** (dotted square), and GdMDOTA$^-$, **5a** (dotted diamond), at 25 °C.

of a series of methylated DOTA ligands, and structural inferences from dipolar shifts alone are not absolutely reliable.

Nuclear Magnetic Relaxation Dispersion and Fluorescence Studies. As shown in Figure 10, the aqueous solutions of the Gd(III) DOTA chelate, **1a**, and of its methylated derivatives display similar S-shaped curves when the relaxivity of the water protons is plotted versus the applied magnetic field or frequency at 25 °C. Nuclear magnetic relaxation dispersion (NMRD) curves such as the ones reproduced in Figure 10 are usually accounted for by the Solomon−Bloembergen equations:[1,2]

$$\frac{1}{T_{1M}} = \frac{10^{-3} q_{H_2O}}{55.5(T_{1M} + \tau_m)} \tag{4}$$

$$\frac{1}{T_{1M}} = \frac{2}{15}\left(\frac{\mu_0}{4\pi}\right)\frac{\hbar^2 \gamma_S{}^2 \gamma_I{}^2 S(S+1)}{r_{Gd-H}{}^6}\left[\frac{3\tau_c}{1+\omega_I{}^2\tau_c{}^2} + \frac{7\tau_c}{1+\omega_S{}^2\tau_c{}^2}\right] \tag{5}$$

where q_{H_2O} is the number of water molecules directly coordinated to the metal ion, r_{Gd-H} is the Gd(III)−water proton distance, and τ_r, τ_m, and τ_s are, respectively, the rotational correlation time, the lifetime of a water molecule in the first coordination sphere, and the longitudinal electronic relaxation time (also labeled T_{1e}). The other parameters have their usual meaning.[1,2] A contribution due to the second coordination sphere must also be taken in consideration.[1,2] The Solomon−Bloembergen equations have been discussed in detail in numerous publications.[1,2] Suffice it to mention here that the smallest correlation time is the major contributor to the correlation time τ_c at each magnetic field as the latter depends on the inverse of the three correlation times:

$$\frac{1}{\tau_c} = \frac{1}{\tau_r} + \frac{1}{\tau_m} + \frac{1}{\tau_s} \tag{6}$$

The correlation time τ_r is expected to dominate the relaxivity of rapidly rotating Gd(III) chelates, and simple S-shaped NMRD curves should be obtained with a dispersion when $\omega_I^2\tau_c^2 \approx 1$. It should also be noted that the electronic relaxation time τ_s depends on the static and the transient zero field splitting (ZFS).[36,37] A correlation time τ_v accounts for the fluctuations of the transient ZFS due to vibrations and intramolecular processes. Differences between the relaxivities of small Gd(III) chelates at low fields could be due to changes of ZFS modulation correlation times.[1,2]

Similar S-shaped NMRD curves are expected for GdDOTA$^-$ and for the chelates investigated here possibly with some differences due to the larger size and the higher rigidity of the polymethylated derivatives. Moreover, GdMDOTA$^-$ is totally asymmetric while the other methylated chelates are highly symmetric species. The methylated DOTA chelates are not the ideal candidates for the observation of strong relaxation effects due to differences of rigidity or symmetry because the rotational correlation time is the major contributor to the relaxivity of these rapidly rotating complexes especially at high fields. Significant relaxivity differences could, however, be observed at low fields because transient ZFS comes into play as noted in earlier reports.[1,2,5] No relaxivity differences that could easily be assigned to symmetry effects could be observed in Figure 10. Small differences in relaxivity at low fields also do not appear to be directly related to a larger molecular volume or to a higher rigidity. For instance, GdMDOTA$^-$ and GdM4DOTMA$^-$ display nearly identical NMRD curves despite differences in size as expected from the ratio between their respective Connolly[38] solvent-excluded volumes (approximately 1.4). It has already been reported that GdDOTA and GdDOTMA have nearly identical NMRD profiles.[43] The rigidity of the macrocyclic cage also does not seem to have an influence on the relaxivity. The lanthanide DOTA chelates are quite rigid with only about 100 inversions of conformation per second at 25 °C.[15] Conformational rearrangements of the tetraaza cycle or of the acetate arms or of both are prevented by the substitution with methyl groups, and the macrocyclic cages become progressively more rigid as methyl substituents are added. However, these intramolecular rearrangements are clearly much too slow to have any influence on the transient ZFS modulation that is taking place at a much faster rate, in the nanoscale range.[37,39] Rigidity could also bring about a lengthening of τ_v as it limits the distortions undergone by the metal chelates when they collide with solvent molecules. Such an effect is not observed in the present case. Predicting a trend in τ_v values when comparing Gd(III) complexes remains open to question despite recent progress in interpreting EPR spectra quantitatively: similar τ_v and vibrational activation energy values have been obtained recently for Gd(H$_2$O)$_8^{3+}$ and for much more rigid Gd(III) chelates.[37,39] Also,

(36) Rast, S.; Fries, P. H.; Belorizky, E.; Borel, A.; Helm, L.; Merbach, A. E. *J. Chem. Phys.* **2001**, *115*, 7554−7563.
(37) Rast, S.; Fries, P. H.; Belorizky, E. *J. Chem. Phys.* **2000**, *113*, 8724−8735.
(38) Connolly, M. L. *J. Appl. Crystallogr.* **1983**, *16*, 548−558.
(39) Rast, S.; Borel, A.; Helm, L.; Belorizky, E.; Fries, P. H.; Merbach, A. E. *J. Am. Chem. Soc.* **2001**, *123*, 2637−2644.

similar values of τ_s were recently reported for GdDOTMA$^-$, **4a**, and GdM4DOTA$^-$, **2a**.[40]

As stated in a recent review,[1] the relaxivity curves of rapidly rotating Gd(III) complexes depend on so many parameters and are so featureless that quantitative interpretations without independent determination of at least some factors are essentially meaningless. An additional difficulty in the present case is the simultaneous presence of several species in solution. As expected, a best fit interpretation of the NMRD curves collected in Figure 10 yields parameters that are close to those reported for GdDOTA$^-$, but no reliable trends could be found when comparing the various chelates (if the τ_m value of GdDOTA$^-$ [41] or GdDOTMA$^-$ [43] are used with $q_{water} = 1$ for all ligands, $\tau_{s0} = 120-250$ ps, $\tau_v = 2-4$ ps, and $\tau_r = 75-250$ ps). No attempts was made at independently determining factors such as τ_m, but the hydration number q_{water} of Tb(III) chelates was determined by a luminescence technique.[13] The progressive crowding of the DOTA structure brought about by the addition of methyl groups results in a decrease of the apparent measured q_{water} from 1.05 for TbDOTA$^-$ to 0.80, 0.76, and 0.62 for TbDOTMA$^-$,[33] TbM4DOTA$^-$, and TbM4DOTMA$^-$, respectively (Table T3 in the Supporting Information), but has little or no influence on the relaxivity, as shown. One could argue that TbM4DOTMA$^-$ is involved in a fast equilibrium between a hydrated and an unhydrated form, but a more likely explanation of the low q_{H_2O} values is that the Gd(III)−water distance becomes larger when the DOTA structure is crowded by methyl substituents. Recent crystallographic studies[42] on macrocyclic lanthanide tetraaza tetraphosphinates showed that the radius contraction of the metal ions is sufficient to bring about an elongation of the metal−O_{water} distance to the point that the hydration water molecule is no longer in the first coordination sphere. The measurement of the hydration state by luminescence is based on the assumption that all Tb(III)−O_{water} distances are identical, but this requirement is probably not fulfilled for the polymethylated DOTA chelates, hence their apparent lower hydration states and possibly faster water exchange times τ_m. Adjusting τ_m could be vital if a small chelate is rigidly associated with a slowly tumbling macromolecule.[1]

Acknowledgment. The authors are grateful to Prof. R. Muller (University of Mons-Hainaut, Belgium) for his help in recording some of the NMRD curves. J.F.D. and V.J. gratefully acknowledge the Fonds National de la Recherche Scientifique and the Institut Interuniversitaire des Sciences Nucléaires of Belgium for their financial support. V.J. is Chercheur Qualifié at the FNRS. J.F.D. and V.J. also thank the EC COST Action D18 "Lanthanide Chemistry for Diagnosis and Therapy" and the EC Florence Large Scale Facility PARABIO for support.

Supporting Information Available: Tables T1−T3 with conditions of synthesis and analytical data and 14 figures S1−S14 with ^{1}H and ^{13}C spectra of metal complexes. This material is available free of charge via the Internet at http://pubs.acs.org.

IC025695E

(40) Atsakin, V. A.; Demidov, V. V.; Vasneav, G. A.; Odintsov, B. M.; Belford, R. L.; Radüchel, B.; Clarkson, R. B. *J. Phys. Chem. A* **2001**, *105*, 9323−9327.

(41) Powell, D. H.; Ni Dhubhghaill, O. N.; Pubanz, D.; Helm, L.; Lebedev, Y. S.; Schlaepfer, W.; Merbach, A. E. *J. Am. Chem. Soc.* **1996**, *118*, 9333−9346.

(42) Lukes, I.; Kotek, J.; Vojtisek, P.; Hermann, P. *Coord. Chem. Rev.* **2001**, *216−217*, 287−312.

(43) Woods, M.; Aime, S.; Botta, M.; Howard, J. A. K.; Moloney, J. M.; Navet, M.; Parker, D.; Port, M.; Rousseaux, O. *J. Am. Chem. Soc.* **2000**, *122*, 9781−9792.